Journal of Materials Chemistry B

PAPER

View Article Online
View Journal | View Issue

Cite this: J. Mater. Chem. B, 2016, 4, 6581

Maleimide-bearing nanogels as novel mucoadhesive materials for drug delivery†

Prasopchai Tonglairoum,[ab] Ruairí P. Brannigan,[a] Praneet Opanasopit[b] and Vitaliy V. Khutoryanskiy*[a]

Received 20th August 2016,
Accepted 20th September 2016

DOI: 10.1039/c6tb02124g

www.rsc.org/MaterialsB

Novel maleimide-functionalised nanogels have been synthesised *via* the polymerisation of 2,5-dimethylfuran-protected 3-maleimidoethyl butylacrylate in the presence of presynthesised poly(*N*-vinylpyrrolidone) (PVP) nanogel scaffolds using surfactant-free emulsion polymerisation techniques. The protected maleimide nanogels were subsequently deprotected to generate the reactive maleimide group *via* a retro-Diels–Alder reaction. These activated nanogels were found to exhibit excellent mucoadhesive properties on *ex vivo* conjunctival tissue when compared to the known mucoadhesive chitosan. In order to determine the viability of the materials as drug carriers, nanogels were loaded with a model drug compound and the *in vitro* release kinetics were analysed. The nanogels could sustain the release of a model drug compound over several hours owing to the swellable hydrophilic nanogel structure, exhibiting first order release kinetics. As a consequence, these findings support the potential of these maleimide-bearing nanogels as a novel platform for sustained drug delivery.

Introduction

Nanogels are defined as nanosized hydrogel materials which consist of networks of chemically or physically cross-linked polymers with sizes up to a few hundred nanometres which can be swollen in aqueous environments.[1,2] Nanogels combine the desirable characteristics of both hydrogel and nano-sized materials, which enables them to exhibit a large surface area, high water content, high aqueous dispersibility, a well-defined structure, tunable chemical and physical structures, good mechanical properties and biocompatibility.[3,4] Moreover, nanogels are capable of encapsulating and releasing high dosages of therapeutic agents.[4,5] As a result, nanogels are ideal candidates for biomedical applications in areas such as sustained drug delivery, imaging and sensing, *etc.*[5–7]

The concept of mucoadhesion has attracted considerable attention in pharmaceutical science in recent decades.[8–12] Mucoadhesion is defined as the ability of a material to adhere to the mucus gel layer, which is an essential criterion in the development of a mucoadhesive drug delivery system.[12] Adhesion between polymeric materials and the mucosal layer has been investigated as a means for prolonging residence times of delivery vehicles at the site of application or absorption, therefore, providing an improvement in drug bioavailability and therapeutic effects.[13,14] Recently, numerous mucoadhesive drug delivery systems have been established for systemic and local delivery through various mucosal tissues such as buccal, nasal, ocular, genitourinary, *etc.*[15–18]

A number of polymers have been shown to possess mucoadhesive capabilities as a consequence of their ability to generate interactions with mucin glycoproteins through physical and/or non-covalent bonds such as hydrogen bonds, van der Waals forces, ionic interactions and chain entanglement.[19] However, in recent years, many studies have attempted to enhance the mucoadhesive properties of materials by modifying polymers to bear specific covalent bond forming functional groups.[20–22] Examples of such functionalities are acrylates,[19] thiols[20] and catechols.[23]

Recently, Mantovani *et al.*[24] reported the use of maleimide functional groups as reactive chain-ends owing to their high reactivity and selectivity towards cysteine residues present at protein surfaces *via* a Michael-type addition reaction.[25] Maleimides exhibit greater reactivity, in terms of C=C bond reactivity, in comparison to fumarates, maleates or acrylates.[26] The withdrawing effects of two activating carbonyls, as well as the discharge of ring strain upon product formation, provide a massive driving force for thiol–maleimide reactions.[27] Thiol–maleimide reactions have been extensively used for bioconjugation owing to their reliability, efficiency and selectivity.[28] Furthermore, maleimide-bearing materials have been found to exhibit a good degree of

[a] School of Pharmacy, University of Reading, Reading, RG6 6UR, UK. E-mail: v.khutoryanskiy@reading.ac.uk
[b] Pharmaceutical Development of Green Innovations Group (PDGIG), Faculty of Pharmacy, Silpakorn University, Nakhon Pathom, Thailand

† Electronic supplementary information (ESI) available: FT-IR and ^{1}H NMR spectra and TGA thermograms of monomers and nanogels, equations for maleimide content and drug loading calculations, release kinetics and statistical analysis. See DOI: 10.1039/c6tb02124g

biocompatibility with a minimal effect on physical properties.[29] Recently, there has been increasing interest in exploiting thiol–maleimide reactions in materials synthesis.[30] Maleimide-bearing nanogels offer a unique platform to improve the mucoadhesive properties of these delivery vehicles.

Herein, we describe the utilisation of a previously synthesised monomer bearing a pendant furan-protected maleimide group to yield nanogel particles using surfactant-free emulsion polymerisation techniques in the presence of a presynthesised poly(*N*-vinylpyrrolidone) (PVP) nanogel 'scaffold'. The nanogels were subsequently deprotected to obtain the active maleimide functional groups on their surface, which were found to exhibit excellent mucoadhesive properties on the ocular mucosal tissues. To the best of our knowledge, the use of maleimide functional groups to enhance the mucoadhesive properties of polymers has not previously been reported.

Experimental

Materials

Maleic anhydride, ethanolamine and acryloyl chloride were purchased from Alfa Aesar (UK). *N*-Vinyl pyrrolidone (NVP), triethylamine, *N*,*N*-methylenebis(acrylamide) (MBA), FITC-dextran (M_W = 10 kDa), fluorescein sodium 2,2′-azobis(2-methylpropionamidine)hydrochloride (V-50), 2,2′-azobis(2-methylpropionitrile) (AIBN), 5,5-dithiobis(2-nitrobenzoic acid) (DTNB), chitosan (62 kDa, 70% deacetylation) and cysteine hydrochloride were purchased from Sigma-Aldrich (UK). All other reagents and solvents were of analytical grade and were used without further purification unless otherwise stated. Simulated tear fluid was composed of NaCl (0.67 g), $NaHCO_3$ (0.20 g), and $CaCl_2{\cdot}2H_2O$ (0.008 g) dissolved in deionized water (100 mL).[1] Whole bovine eyeballs were sourced from a local abattoir on the day of slaughter, and transported in phosphate buffer (pH 7.4) maintained at 4–8 °C. The conjunctival tissues were removed and washed using phosphate buffer. All tissues were used within 24 h of retrieval.

Synthesis of 2,5-dimethylfuran-protected anhydride (1)

The following procedures were modified from previous studies of Mantovani *et al.*[24] and Syrett *et al.*[30] Briefly, in a clean two-necked round-bottom flask fitted with a condenser, a stirrer bar and a septum, maleic anhydride (30 g, 306 mmol) was dissolved in toluene (150 mL) and heated to reflux. Using a syringe, furan (33.4 mL, 459 mmol) was slowly added and reaction was allowed to proceed overnight. Subsequently, the reaction mixture was allowed to cool to ambient temperature (25 °C) to yield the product as a white solid which was retrieved by filtration and washed with petroleum ether. Yield: 79%. ^{1}H NMR (400 MHz, DMSO-d_6) δ 3.29 (s, 2H, C*H*), 5.33 (s, 2H, C*H*), 6.56 (s, 2H, C*H*) (Fig. S1, ESI†).

Synthesis of 2,5-dimethylfuran-protected 3-maleimido ethyl alcohol (2)

Employing the same apparatus previously used, furan protected anhydride (**1**) (15.5 g, 93 mmol) was suspended in 400 mL of methanol and cooled using an ice-bath for 30 min before the addition of triethylamine (13 mL, 98.47 mmol) with stirring. To the cooled reaction mixture, ethanolamine (6.2 mL, 102.52 mmol) was added dropwise with rigorous stirring and was allowed to stir for 10 min before subsequently being warmed to room temperature for 30 min, and finally, heated to reflux (75 °C) for 18 h. In order to maximise conversion, after the reaction was complete, a further 1 mL of ethanolamine was added and the reaction was allowed to proceed for a further 2 h. The reaction mixture was then cooled to room temperature and the product precipitated as white crystalline powder which was collected by filtration and washed with isopropyl alcohol (IPA). Yield: 34%. ^{1}H NMR (400 MHz, DMSO-d_6) δ 2.93 (s, 2H, C*H*), 3.42 (m, 4H, $(CO)_2NCH_2$–CH_2OH), 4.79 (s, 1H, O*H*), 5.12 (s, 2H, C*H*), 6.55 (s, 2H, C*H*) (Fig. S2, ESI†).

Synthesis of 2,5-dimethylfuran-protected 3-maleimidoethyl butylacrylate (3)

In a clean dry round-bottom flask fitted with a stirrer bar and flushed with N_2, furan-protected maleimide alcohol (**2**) (5.0 g, 24 mmol) was suspended in 100 mL of dichloromethane (DCM) before the addition of triethanolamine (4.2 mL, 31.8 mmol). The solution was cooled using an ice bath for 30 min, after which acryloyl chloride (4.3 mL, 53.2 mmol) was added dropwise with vigorous stirring. The reaction was allowed to proceed for 2 h before the reaction mixture was warmed to room temperature for 24 h. The reaction mixture was filtered to remove any salt product produced during the reaction and the filtrate was extracted with 1 M NH_4Cl (500 mL), deionised water (500 mL) and brine (500 mL). The organic phases were combined and the solvent was removed *via* rotary evaporation to yield the product as a pale yellow oil. Yield: 67%. ^{1}H NMR (400 MHz, DMSO-d_6) δ 2.95 (s, 1H, C*H*), 3.66 (t, $^3J_{H-H}$ = 5.5 Hz, 2H, $(CO)_2NCH_2$–), 4.18 (t, $^3J_{H-H}$ = 5.5 Hz, 2H, –CH_2OCO), 5.12 (s, 2H, C*H*), 6.93–6.30 (m, 3H, C*H*=CH_2), 6.55 (s, 2H, C*H*) (Fig. S3, ESI†).

Synthesis of poly(vinylpyrrolidone) (PVP) nanogels

PVP nanogels were prepared using a modified procedure from the study of Yang *et al.*[31] Briefly, 200 mL of deionised water was added to a round-bottom flask and deoxygenated by stirring under nitrogen bubbling for 20 min. After purging, the monomer mixture, *N*-vinylpyrrolidone (NVP) (2.5 g, 22.5 mmol) and methylene bis-acrylamide (MBA) (0.25 g, 1.6 mmol) in 5 mL of chloroform, was added followed by the initiator V-50 (2.5 mg, 9.2 μmol). The polymerisation mixture was heated to 70 °C and polymerisation allowed to proceed for 18 h at 400 rpm stirring. The PVP nanogels were subsequently purified by dialysis against deionised H_2O before lyophilisation. The nanogels were stored at 4–8 °C under nitrogen before use.

Synthesis of furan-protected maleimide-PVP (pMal-PVP) nanogels

In a clean round-bottom flask, 200 mL of deionised H_2O was bubbled with nitrogen for 20 min before the addition of the azo-initiator AIBN (27.5 mg). PVP nanogels (250 mg), MBA (275 mg) and the furan-protected maleimide acrylate monomer (**3**) (2.50 g) were dissolved in chloroform (5 mL) before being

added to the deoxygenated initiator solution. The polymerisation mixture was heated to 70 °C and the polymerisation was allowed to proceed for 6 h under N_2 at 400 rpm stirring. The opaque solution of nanogels was then cooled and purified by dialysis against deionized H_2O before lyophilisation. The nanogels were stored at 4–8 °C under nitrogen before use.

Synthesis of free maleimide-PVP (Mal-PVP) nanogels

The deprotection of the furan-protected maleimide groups was performed using a retro-Diels–Alder reaction to yield free maleimide groups. Briefly, 50 mg of protected pMal-PVP nanogels were dispersed in toluene (50 mL) and heated to reflux for 18 h. The mixture was subsequently cooled and toluene was removed *in vacuo*. Deprotected Mal-PVP nanogels were dialysed against DMSO followed by deionised H_2O before lyophilisation, in order to remove trace toluene and furan. The Mal-PVP nanogels were stored at 4–8 °C before use.

Determination of maleimide group content

To determine the maleimide content of the nanogels, Mal-PVP nanogels were first reacted with a known amount of excess thiol and then the remaining unreacted thiol was quantified using Ellman's assay.[32] Briefly, the deprotected nanogels (30 mg) were placed in a 5 mL glass vial containing a solution of cysteine·HCl (3 mg, 19 μmol) dissolved in a phosphate buffer solution (0.5 M, pH 8). The nanogels were allowed to swell and react for 1 h after which the nanogels were separated from the aqueous solutions by centrifugation at 13 000 rpm for 10 min. The supernatant liquid was determined for the remaining thiol using Ellman's reagent, 5,5-dithio-bis-(2-nitrobenzoic acid) (DTNB). Ellman's reagent or DTNB (3 mg, 7.6 μmol) was dissolved in 10 mL of phosphate buffer solution (0.5 M, pH 8). Then 500 μL of DTNB stock solution was added to 500 μL of the supernatant liquid and incubated in the dark for 2 h. The absorbance of the mixture was determined using an Epoch Microplate Spectrophotometer microplate reader at λ = 420 nm. The unreacted thiol was quantified using a calibration curve of cysteine hydrochloride prepared as a series of solutions, with a concentration range of 0.018–0.797 μmol mL^{-1}, prepared under the same conditions. The cysteine solution without being mixed with the nanogels was used as a control. The quantity of free maleimide present in the Mal-PVP nanogels is calculated as the difference between the initial amount of thiol and the amount of unreacted thiol after the complete reaction of all maleimide groups (eqn (S1), ESI†).

Model drug loading of Mal-PVP nanogels

In order to demonstrate the applicability of the nanogels for drug delivery, fluorescein sodium was employed as a model compound to load into the nanogel using an adsorption method. Briefly, lyophilised Mal-PVP nanogels (30 mg) were added to a 2 mL aqueous solution of fluorescein sodium (2 mg mL^{-1} in deionised H_2O) and subsequently mixed using a rotary mixer. After 48 h, the nanogels were removed from solution by centrifugation at 13 000 rpm for 10 minutes. The amount of free fluorescein sodium in the supernatant was measured by using a Varian Cary Eclipse fluorescence spectrometer at the excitation and emission wavelengths of λ = 460 and 512 nm, respectively, and the encapsulation efficiency (eqn (S2), ESI†) and loading capacity (eqn (S3), ESI†) were determined.

Mucoadhesion of nanogels on *ex vivo* bovine conjunctival mucosa

The mucoadhesive properties of the nanogels on bovine conjunctival mucosa were determined using a method modified from previous work done within the group.[33] Aqueous solutions of deprotected nanogels (1 mg mL^{-1} in deionised H_2O), protected nanogels (1 mg mL^{-1} in deionised H_2O), chitosan (1 mg mL^{-1} in 0.5% acetic acid) and dextran (1 mg mL^{-1} in deionised H_2O) were prepared and loaded with fluorescein sodium (0.5 mg mL^{-1}, procedure for nanogel loading later described) in simulated tear fluid. Free fluorescein sodium was dissolved in deionised water and added to viscous solutions of chitosan and dextran in simulated tear fluid with stirring until a homogeneous gel was achieved. The pH of chitosan solution was adjusted to 6 using 1% NaOH. An aliquot (20 μL) was pipetted onto a 1 × 1 cm^2 piece of *ex vivo* conjunctival mucosa, which was then placed onto a sloped channel, and washed with simulated tear fluid using a syringe pump (200 μL min^{-1}). At pre-determined intervals, fluorescence images of the whole tissue were taken using a Leica MZ10F fluorescence stereomicroscope fitted with a GFP filter. The fluorescence images were then analysed using ImageJ software by measuring the pixel intensity of the images, which was linearly correlated with the concentration of nanogels present. The pixel intensity of the blank samples (conjunctival mucosa without nanogels present) was deducted from each measurement. The data were presented as a percent of nanogels remaining on the mucosa surface with elution time. The experiments were conducted in triplicate.

In vitro release from Mal-PVP nanogels

The *in vitro* release of fluorescein sodium from loaded nanogels was studied using a dialysis method modified from previously reported work.[34] Briefly, 2 mL of fluorescein sodium-loaded nanogels in simulated tear fluid (7.5 mg mL^{-1}) was contained in a Pur-A-Lyzer™ Maxi 3500 dialysis kit. The dialysis kit was submerged in 30 mL of simulated tear fluid (pH 7.4) that was incubated at 35 °C and shaken at 80 rpm for 24 h. At given intervals, 5.0 mL aliquots of the release medium were withdrawn and replaced with fresh medium to maintain a constant volume. The released fluorescein sodium in each aliquot was determined by fluorescence spectroscopy at excitation and emission wavelengths of λ = 460 and 512 nm, respectively. The experiments were conducted in triplicate and the release kinetics of fluorescein sodium from the nanogels were also calculated using the zero-order model, the first-order model and the Higuchi model.

Results and discussion

Synthesis of pMal-PVP and Mal-PVP nanogels

In agreement with previous studies, 2,5-dimethylfuran-protected 3-maleimidoethyl butylacrylate (3) was synthesised in reasonable

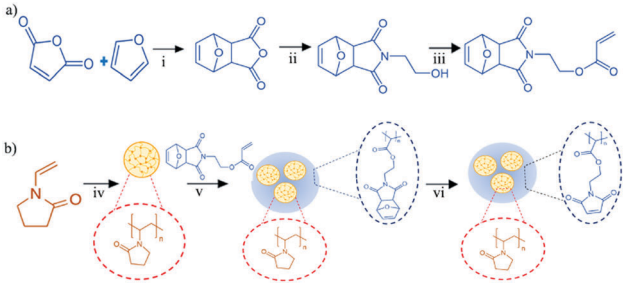

Fig. 1 (a) Synthetic route of the protected maleimide monomer; (i) toluene, reflux, 18 h. (ii) Ethanolamine, triethanolamine, MeOH, 0 °C to 75 °C, 18 h. (iii) Acryloyl chloride, triethanolamine, DCM, 0 °C to 25 °C, 24 h. (b) Nanogel synthesis and deprotection to activate maleimide groups: (iv) MBA, NVP, deionised H_2O, 70 °C, 18 h. (v) Monomer (**3**), PVP nanogels, MBA, deionised H_2O, 70 °C, 6 h. (vi) Protected maleimide nanogels, toluene, 110 °C, 18 h.

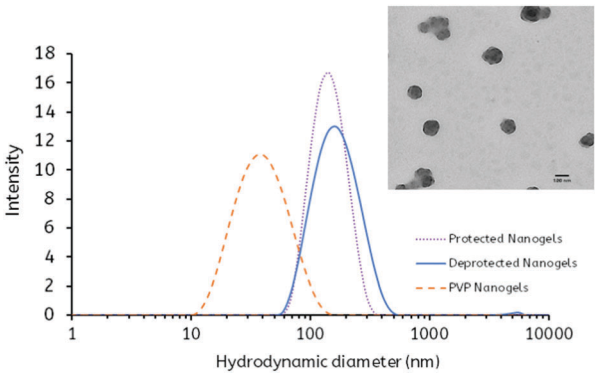

Fig. 2 Hydrodynamic diameter of PVP nanogels, protected nanogels and deprotected nanogels as determined by dynamic light scattering. Inset: TEM image of the Mal-PVP nanogels (20 000×). The scale bar is 100 nm.

yields with minimal purification needed (Fig. 1(a)). The ^{1}H NMR spectrum of the protected monomer exhibited a multiplet between 5.93 and 6.30 ppm which is highly characteristic of acrylate formation. Furthermore, the complete loss of the triplet at 4.79 ppm, attributed to the free alcohol of the pre-monomer (**2**), and the appearance of a triplet at 4.18 ppm, attributed to the CH_2 adjacent to the acrylate group, are indicative of complete acrylation (Fig. S2 and S3, ESI†). In addition, the presence of singlets at 2.95, 5.12 and 6.55 ppm indicates the retention of the furan protecting group.

PVP nanogels were prepared using a surfactant-free emulsion polymerisation technique previously reported in the literature.[31] The successful synthesis of the nanogels was verified by ^{1}H NMR and FT-IR spectroscopy, whilst the hydrodynamic diameter, size distribution and colloidal stability were determined by dynamic light scattering (DLS).

In agreement with previous studies, the ^{1}H NMR spectrum exhibited the characteristic PVP peaks attributed to the protons of the carbon backbone (1.43–1.7 ppm and 3.8 ppm) in addition to peaks attributed to the pyrrolidone side group (2.0, 2.4 and 3.2 ppm) (Fig. S4, ESI†). Furthermore, the FT-IR spectrum displayed absorption bands at 1647, 1427 and 1288 cm^{-1} that correspond to the C=O group, C–H bending vibration and C–N stretching vibration, respectively, typical of PVP (Fig. S5, ESI†). The DLS analysis revealed that the synthesis yielded nanogels which displayed a monodisperse size distribution (PDI = 0.21) with a mean hydrodynamic diameter of 45 ± 1 nm. Furthermore, the PVP nanogels displayed a reasonable colloidal stability, exhibiting a ζ-potential = −15.08 ± 3.36 mV (Fig. 2 and Table 1).

After synthesis, the PVP nanogels were utilised as a nanogel 'scaffold' for the polymerisation of the protected maleimide monomer, using MBA as a crosslinker, to produce 'core–shell' type protected maleimide-bearing (pMal-PVP) nanogels (Fig. 1(b)). As with the PVP nanogel 'scaffolds', the core–shell type nanogels were analysed *via* ^{1}H NMR and FT-IR spectroscopy and DLS. The ^{1}H NMR spectrum of the pMal-PVP nanogels displayed singlet peaks at 6.51, 5.26 and 2.90 ppm characteristic of the protons of the Diels–Alder adduct, confirming the retention of the furan protecting groups (Fig. 3(a)).

Furthermore, the retention of the characteristic PVP peaks previously described is indicative of the di-polymeric system. This is corroborated by the FT-IR spectrum through the presence of absorption bands that are attributable to both the protected maleimide and PVP components, namely, the absorption bands at 1170 and 1695 cm^{-1} attributed to C=O stretching vibration of maleimide (Amide I), bands at 1186 and 1019 cm^{-1} attributed to the C–O–C and C=C stretching vibration of the furan ring respectively, and a band at 1647 cm^{-1} corresponding to the C=O group of PVP (Fig. S5, ESI†).

Recently, thermogravimetric analysis (TGA) was employed to further verify the presence of two polymeric species. The TGA thermograms verified that the nanogels consisted of two components, with two major thermal degradation temperatures of 150 and 380 °C, corresponding to the decomposition of the pMal layer and the PVP 'scaffold', respectively (Fig. S6, ESI†).

Interestingly, the DLS analysis revealed that after copoly merisation of the PVP nanogel scaffolds with the 2,5-dimethyl-furan-protected 3-maleimidoethyl butylacrylate monomer, the hydrodynamic diameter increased substantially (d = 134 ± 1 nm), with a large reduction in the PDI value (PDI = 0.09) (Table 1 and Fig. 2). It is proposed that this may be attributed to the aggregation of the PVP nanogels during the polymerisation in order to stabilise the relatively hydrophobic protected maleimide polymer. In addition to this, it was found that the zeta potential of the pMal-PVP nanogels also decreased (ζ-potential = −19.43 ± 3.53 mV), indicative of a higher degree of colloidal stability.

To 'activate' the maleimide functional groups on the nanogels, the furan protecting group was removed *via* a retro-Diels–Alder reaction (Fig. 1(b)). After deprotection, the ^{1}H NMR spectrum of the Mal-PVP nanogels showed the complete loss of the singlets at 5.12 and 6.55 ppm, characteristic of the Diels–Alder adduct, and the formation of a singlet at 7.01 ppm which is attributed to the protons of the deprotected maleimide (Fig. 3). Additionally, the FT-IR spectrum reveals the disappearance of the absorption bands at 1186 and 1019 cm^{-1} that were assigned to the C–O–C and C=C band of the furan ring in conjunction with the appearance of a band at 833 cm^{-1}, corresponding to the =CH wag vibration of the free maleimide (Fig. S5, ESI†). The appearance

Table 1 Physicochemical features of PVP, pMal-PVP and Mal-PVP nanogels

Nanogel	Size (nm)	PDI	Zeta potential (mV)	Yield (%)	Maleimide content (μmol g^{-1})
PVP	45 ± 1	0.21 ± 0.01	−15.08 ± 3.36	68	N/A
Protected	134 ± 1	0.09 ± 0.01	−19.43 ± 3.53	37	N/A
Deprotected	152 ± 1	0.15 ± 0.02	−20.41 ± 1.10	88	323.47 ± 2.04

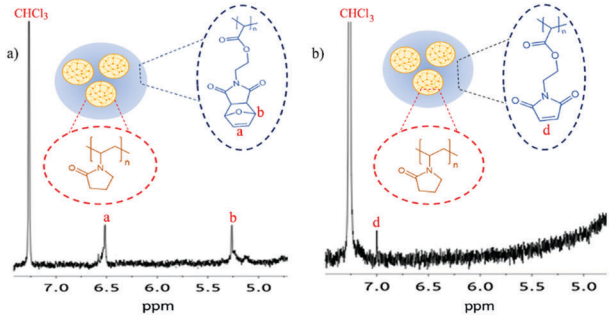

Fig. 3 ^{1}H NMR spectra of the nanogels (a) prior to deprotection and (b) after deprotection in $CHCl_3$ (400 MHz, 25 °C, $CDCl_3$). Inset: The structure of the nanogels before and after deprotection.

of new peaks together with changes in existing peaks in both the ^{1}H NMR and FT-IR spectra is highly indicative of the successful activation of the maleimide moiety.

As predicted, owing to an increase in hydrophilicity, it was found by DLS that the hydrodynamic diameter of the nanogels increased significantly upon deprotection (d = 152 ± 1 nm) (Fig. 2 and Table 1). Furthermore, an additional decrease in the zeta potential is observed (ζ-potential = −20.41 ± 1.10 mV), suggesting an improvement in colloidal stability, typical of these hydrophilic systems (Table 1). It is important to note that only a small decrease in zeta potential was observed as a consequence of the loss of the relatively neutral, in terms of charge potential, furan protecting group.

Determination of maleimide group content

As a consequence of the high reactivity of the maleimide moiety towards the cysteine subunit of mucins, the Mal-PVP nanogels were expected to have strong mucoadhesive properties. In order to determine the quantity of maleimide groups available for mucosal binding, a reverse Ellman's assay was conducted.[35] In this procedure, the nanogels were first reacted with a known amount of excess thiol and then the remaining unreacted thiol was determined *via* a traditional Ellman's assay. The amount of maleimide is computed as the difference between the initial amount of thiol and the amount of unreacted thiol after the complete reaction of all maleimide groups (eqn (S1), ESI†). The result showed that the available maleimide content of the Mal-PVP nanogels was 323.47 ± 2.04 μmol g^{-1} of nanogels (Table 1). Furthermore, it was found that both the PVP and pMal-PVP exhibited no free maleimide as expected. In comparison with other mucoadhesive nanogels synthesised by the group, namely thiolated nanogels, the content of mucoadhesive functionality per gram of nanogel is relatively high and offers a suitable platform for mucoadhesion while negating stability issues associated with thiol-bearing materials, namely oxidation.[34]

Model drug loading of Mal-PVP nanogels

In order to demonstrate the potential of the maleimide bearing nanogels for drug delivery application, fluorescein sodium was used as both a model drug compound and a fluorescent 'tag' for analysis of mucoadhesive properties. The fluorescein was loaded into the nanogels using the adsorption method by straightforwardly incubating the nanogels in an aqueous solution of fluorescein sodium. It was found by fluorescence spectrometry that the loading efficiency of the Mal-PVP nanogels was ≈15%, with a maximum loading capacity = 21 μg mg^{-1} of Mal-PVP nanogels.

Mucoadhesive properties of the nanogels

In order to assess the mucoadhesive properties of the Mal-PVP nanogels, the retention of fluorescein loaded on *ex vivo* bovine conjunctival tissue was assessed using fluorescence microscopy (Fig. 4). Chitosan and dextran were employed as a positive control and a negative control, respectively, based on previous studies, however, it is important to note that a direct comparison between materials is not possible as a consequence of chitosan and dextran being linear polymers.[36,37] In addition, the mucoadhesive properties of the protected pMal-PVP nanogels were also assessed in order to demonstrate the effect of free maleimide on the mucoadhesive capabilities of the nanogels. After pixel analysis of the images obtained from fluorescence microscopy,

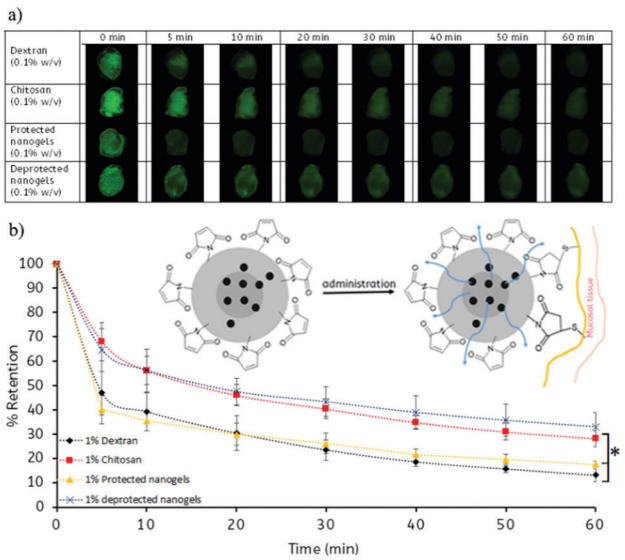

Fig. 4 (a) Exemplar fluorescence images of conjunctival tissue after washing. (b) Percentage retention of deprotected nanogels, protected nanogels, chitosan and dextran on the surface of *ex vivo* bovine conjunctival tissue. Data are expressed as mean ± standard deviation (n = 3). * Statistically significant difference ($P < 0.05$).

it was found that the deprotected nanogels exhibited excellent mucoadhesive properties which were comparable to the mucoadhesive properties of chitosan. It was found that 33% of the Mal-PVP nanogels were retained on the conjunctival tissue after 1 h of washing as compared to 28% of chitosan. Although their % retention was found not to be statistically significantly, different from chitosan, the mucoadhesive properties of these maleimide bearing materials show a major advancement in the field of mucoadhesive polymers.

Furthermore, the control experiment investigating the mucoadhesive properties of the protected pMal-PVP nanogels revealed that without the presence of free maleimide groups, the nanogels displayed a statistically significant lower retention capability compared to the Mal-PVP nanogels ($p < 0.05$) (Tables S1 and S2, ESI†). It was found that only 17% of the pMal-PVP nanogels remained on the tissue after 1 h of washing. These experiments confirm the desirable mucoadhesive properties of the deprotected nanogels which can potentially be used as mucoadhesive drug carriers. Moreover, these maleimide bearing nanogels may be considered as a novel class of mucoadhesive materials.

In vitro release from Mal-PVP nanogels

The *in vitro* release studies of fluorescein sodium from loaded Mal-PVP nanogels were performed in simulated tear fluid (pH 7.4), and the release characteristics were plotted as a function of time (Fig. 5). The release experiment indicated that the fluorescein sodium was gradually released from the nanogels in a time-dependent manner. Consistent with a burst release typical for these systems, the release was found to be faster in the first four hours of the study. In order to improve the efficacy of the drug being delivered, not only the retention of the drug carriers at the site of action is important, but also the capability of the carrier to sustain the release of the drug over a suitable period of time. The release along with mucoadhesion studies indicated that the nanogels could retain and release the drug for a period in excess of 24 h.

Approximately 85% of the fluorescein sodium contained in the nanogels was released into the simulated tear fluid after 24 h. This release profile fits well with the first order kinetics model ($R^2 > 0.99$) (Fig. S7–S9, ESI†) which describes the drug dissolution in pharmaceutical dosage forms containing water-soluble drugs in hydrophilic matrices. This may be a consequence of the hydrophilic Mal-PVP nanogel swelling, resulting in an increased diffusion path length in combination with the reduction concentration dependent diffusion.[38]

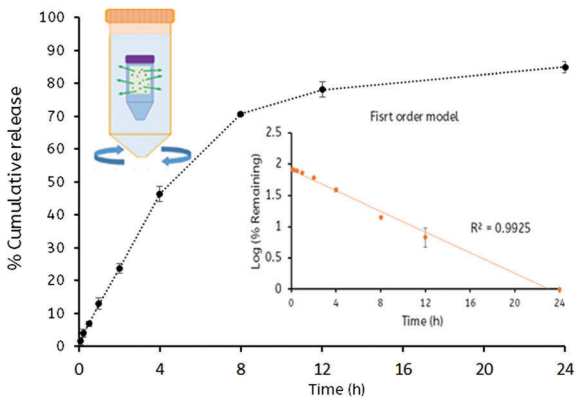

Fig. 5 Release profiles of fluorescein sodium from the nanogels. Data are expressed as mean standard deviation (n = 3). Inset: Schematic illustration of the release experiment (top left) and fitting of the release profile with first order kinetics.

Conclusions

In conclusion, we have reported the first example of maleimide-functionalised polymers being used as mucoadhesive materials. Utilising cost efficient and facile synthetic routes, we have developed a unique, and potentially scalable, platform for the synthesis of maleimide-containing nanogels. Furthermore, the mucoadhesive and loading and release capacities of these materials have been demonstrated and therefore, these nanogels may be promising candidates for controlled drug delivery.

Acknowledgements

Joint first co-authorship is attributed to Prasopchai Tonglairoum and Dr Ruairí P. Brannigan. The authors gratefully acknowledge the Leverhulme Trust for funding (RPG-2013-017), the Commission of Higher Education (Thailand), the Thailand Research Funds through the Golden Jubilee PhD Program (Grant No. PHD/0092/2554) and the Newton-TRF PhD Scholarship for financial support and providing 12-month placement for PT at the University of Reading. Special thanks to Dr Peter Harris for his help with TEM analysis and Dr Samuel C. Bizley for his advice on this work. The Chemical Analysis Facility at the University of Reading is thanked for access to NMR, TGA, FT-IR and TEM.

References

1 H. J. Kao, H. R. Lin, Y. L. Lo and S. P. Yu, *J. Pharm. Pharmacol.*, 2006, **58**, 179–186.
2 S. Maya, B. Sarmento, A. Nair, N. S. Rejinold, S. V. Nair and R. Jayakumar, *Curr. Pharm. Des.*, 2013, **19**, 7203–7218.
3 M. Molina, M. Asadian-Birjand, J. Balach, J. Bergueiro, E. Miceli and M. Calderon, *Chem. Soc. Rev.*, 2015, **44**, 6161–6186.
4 Y. Li, D. Maciel, J. Rodrigues, X. Shi and H. Tomás, *Chem. Rev.*, 2015, **115**, 8564–8608.
5 R. T. Chacko, J. Ventura, J. Zhuang and S. Thayumanavan, *Adv. Drug Delivery Rev.*, 2012, **64**, 836–851.
6 C. Hayashi, U. Hasegawa, Y. Saita, H. Hemmi, T. Hayata, K. Nakashima, Y. Ezura, T. Amagasa, K. Akiyoshi and M. Noda, *J. Cell. Physiol.*, 2009, **220**, 1–7.
7 U. Hasegawa, S.-I. M. Nomura, S. C. Kaul, T. Hirano and K. Akiyoshi, *Biochem. Biophys. Res. Commun.*, 2005, **331**, 917–921.
8 R. Shaikh, T. R. Raj Singh, M. J. Garland, A. D. Woolfson and R. F. Donnelly, *J. Pharm. BioAllied Sci.*, 2011, **3**, 89–100.
9 N. A. Peppas and Y. Huang, *Adv. Drug Delivery Rev.*, 2004, **56**, 1675–1687.
10 A. Sosnik, J. das Neves and B. Sarmento, *Prog. Polym. Sci.*, 2014, **39**, 2030–2075.

11 V. V. Khutoryanskiy, *Mucoadhesive Materials and Drug Delivery Systems*, John Wiley & Sons, Ltd, 2014.
12 V. V. Khutoryanskiy, *Macromol. Biosci.*, 2011, **11**, 748–764.
13 B. M. Boddupalli, Z. N. K. Mohammed, R. A. Nath and D. Banji, *J. Adv. Pharm. Technol. Res.*, 2010, **1**, 381–387.
14 G. P. Andrews, T. P. Laverty and D. S. Jones, *Eur. J. Pharm. Biopharm.*, 2009, **71**, 505–518.
15 T. Schmitz, V. M. Leitner and A. Bernkop-Schnurch, *J. Pharm. Sci.*, 2005, **94**, 966–973.
16 C. Valenta, C. E. Kast, I. Harich and A. Bernkop-Schnurch, *J. Controlled Release*, 2001, **77**, 323–332.
17 J. O. Morales and J. T. McConville, *Eur. J. Pharm. Biopharm.*, 2011, **77**, 187–199.
18 A. Ludwig, *Adv. Drug Delivery Rev.*, 2005, **57**, 1595–1639.
19 M. Davidovich-Pinhas and H. Bianco-Peled, *J. Mater. Sci.: Mater. Med.*, 2010, **21**, 2027–2034.
20 A. Bernkop-Schnürch, *Adv. Drug Delivery Rev.*, 2005, **57**, 1569–1582.
21 A. Bernkop-Schnurch, M. Hornof and T. Zoidl, *Int. J. Pharm.*, 2003, **260**, 229–237.
22 M. Davidovich-Pinhas, O. Harari and H. Bianco-Peled, *J. Controlled Release*, 2009, **136**, 38–44.
23 J. Xu, G. M. Soliman, J. Barralet and M. Cerruti, *Langmuir*, 2012, **28**, 14010–14017.
24 G. Mantovani, F. Lecolley, L. Tao, D. M. Haddleton, J. Clerx, J. J. L. M. Cornelissen and K. Velonia, *J. Am. Chem. Soc.*, 2005, **127**, 2966–2973.
25 S. D. Fontaine, R. Reid, L. Robinson, G. W. Ashley and D. V. Santi, *Bioconjugate Chem.*, 2015, **26**, 145–152.
26 D. P. Nair, M. Podgórski, S. Chatani, T. Gong, W. Xi, C. R. Fenoli and C. N. Bowman, *Chem. Mater.*, 2014, **26**, 724–744.
27 B. H. Northrop, S. H. Frayne and U. Choudhary, *Polym. Chem.*, 2015, **6**, 3415–3430.
28 A. B. Lowe, *Polym. Chem.*, 2010, **1**, 17–36.
29 T. Li and S. Takeoka, *Int. J. Nanomed.*, 2013, **8**, 3855–3866.
30 J. A. Syrett, G. Mantovani, W. R. S. Barton, D. Price and D. M. Haddleton, *Polym. Chem.*, 2010, **1**, 102–106.
31 Q. Yang, K. Wang, J. Nie, B. Du and G. Tang, *Biomacromolecules*, 2014, **15**, 2285–2293.
32 G. L. Ellman, *Arch. Biochem. Biophys.*, 1959, **82**, 70–77.
33 G. S. Irmukhametova, G. A. Mun and V. V. Khutoryanskiy, *Langmuir*, 2011, **27**, 9551–9556.
34 M. T. Cook, S. A. Schmidt, E. Lee, W. Samprasit, P. Opanasopit and V. V. Khutoryanskiy, *J. Mater. Chem. B*, 2015, **3**, 6599–6604.
35 A. Wagh, S. Y. Qian and B. Law, *Bioconjugate Chem.*, 2012, **23**, 981–992.
36 A. Storha, E. A. Mun and V. V. Khutoryanskiy, *RSC Adv.*, 2013, **3**, 12275–12279.
37 G. Prosperi-Porta, S. Kedzior, B. Muirhead and H. Sheardown, *Biomacromolecules*, 2016, **17**, 1449–1457.
38 G. Singhvi and M. Singh, *Int. J. Pharm. Sci. Res.*, 2011, **2**, 77–84.